International Conference on Space Optics—ICSO 2012

Ajaccio, Corse

9–12 October 2012

Polarization scramblers in Earth observing spectrometers: lessons learned from Sentinel-4 and 5 phases A/B1

Jérôme Caron

Jean-Loup Bézy

Grégory Bazalgette Courrèges-Lacoste

Bernd Sierk

et al.

Polarization scramblers in Earth observing spectrometers: lessons learned from Sentinel-4 and 5 phases A/B1

Jérôme Caron, Jean-Loup Bézy, Grégory Bazalgette
Courrèges-Lacoste, Bernd Sierk, Roland Meynart
European Space Agency, ESA-ESTEC
Keplerlaan 1, 2200AG Noordwijk, The Netherlands.

Michael Richert, Didier Loiseaux
EADS Sodern, 20 avenue Descartes, BP23,
94451 Limeil-Brevannes Cedex, France.

Abstract— **Sensitivity to polarization is a major design driver for Earth observing dispersive spectrometers. While the measured Earth radiance observed from space in the UV, visible and near IR bands has a strong and highly variable linearly polarized component, most essential components in spectrometers are inherently sensitive to polarization: scan mirrors, gratings, dichroics. Minimisation of the resulting radiometric errors is a challenge and cannot be only achieved with careful optical designs. Depolarization by passive optical components such as birefringent polarization scramblers has been demonstrated with the last generation of atmosphere monitoring instruments (MERIS, OMI). In order to achieve the demanding performances targeted by future instruments (Sentinel-4, Sentinel-5, CarbonSat) the available degrees of freedom left for optimisation shall be explored, and new polarization scrambler designs must be found.**

This paper summarizes design rules and performance aspects identified by ESA during phases A/B1 of the Sentinel-4 and Sentinel-5 missions. The following aspects have been investigated and will be discussed: minimization of polarization dependent spectral oscillations, use of a polarization scrambler in converging beam or parallel beam at large angles of incidence, polarization dependent pointing error.

Keywords-spectrometer, polarization, depolarizer, scrambler, Sentinel-4, Sentinel-5.

I. INTRODUCTION

In the frame of the GMES (Global Monitoring for Environment and Security) initiative, ESA is supervising the development of two high resolution spectrometers dedicated to the monitoring of the Earth's atmosphere: Sentinel-4 and Sentinel-5. The characteristics of these instruments (called hereafter S4 and S5) are summarized in table 1: S4 is a scanning spectrometer on board the geostationary satellite MTG-S (Meteosat Third Generation - Sounder) scheduled for launch in 2019 [1]; while S5 is a pushbroom instrument that will fly on a low altitude Earth orbit (LEO) on board Metop-SG (Metop Second Generation) planned for launch at the end of 2020.

Comparing to the previous generation of atmosphere monitoring instruments, with SCIAMACHY on board Envisat, and GOME-2 on board Metop, S4 and S5 are targeting notably improved temporal, geometrical, spectral and radiometric performances. It has been early recognized that the demanding instrument characteristics require in particular a high immunity to the polarization of the observed radiation. In the spectral bands of interest extending from 270nm to 2385nm, Rayleigh scattering is a strong source of polarization, although at the largest wavelengths weaker effects such as sunglint, reflection on ice clouds or ground reflection may become more important. Below 1000nm where Rayleigh scattering clearly dominates, the observed polarization is almost perfectly linear and largely imposed by the measurement geometry (between Sun, Earth and satellite). At first order, one can assume that the angle of polarization direction is spectrally constant for a given observation and illumination geometry, and the degree of polarization (DOP) depends on the amount of unpolarized signal coming in but cannot exceed the DOP observed for pure Rayleigh scattering.
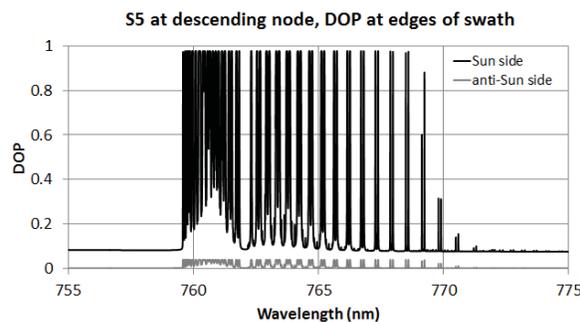

Figure 1. Spectral variations of the degree of polarization (DOP) observed by Sentinel-5 at its descending node, on both edges of the instrument swath. A mid-latitude summer AFGL profile is assumed, with a layer of continental aerosol with optical depth 0.2 located between 900 and 700 hPa, and a ground albedo of about 0.35 representative for healthy vegetation.

A curve showing typical spectral DOP variations in the Oxygen A band is plotted on fig.1, calculated for S5 at its descending node, on both edges of the swath. The polarization is stronger in the absorption bands where the atmosphere is opaque and the strong unpolarized signal from the ground is not visible. Outside the absorbing bands, the ground contribution dominates and lowers the DOP. The anti-Sun side of the swath is close to the backscattering direction, where polarization of Rayleigh scattered light is very low while the Sun side corresponds to a scattering angle close to 90 deg which maximises polarization.

In SCIAMACHY and GOME-2, the approach of measuring polarization was taken with respectively the Polarization Measurement Device (PMD) [2, 3] and the Polarization Unit (PU) [4]. Due to cost and mass constraints, in S4 and S5 passive optical components destroying the incoming polarization such as a polarization scrambler were selected. Polarization scramblers, also called scrambling windows or scramblers in short, are the subject of this paper. They have been implemented in several instruments such as MERIS (on board Envisat) [5], OMI (on board Aura) [6]. They are also considered for OLCI (on board Sentinel-3) and Tropomi (Sentinel-5 precursor mission) instruments.

TABLE I. INSTRUMENTS USING A POLARIZATION SCRAMBLER.

	MERIS	OMI	Sentinel-4	Sentinel-5
Target	Land, Ocean, Atmosphere	Ozone	Atmosphere	Atmosphere
Platform	Envisat	Aura	MTG-S	Metop-SG
Overview	Medium resolution pushbroom, 5 cameras in fan shape	High resolution pushbroom	High resolution, E-W scan mirror	High resolution pushbroom
Pupil	Close to rectangular 40*20 mm^2	Rectangular 7.6*5.6 mm^2	Circular 95 mm diameter	Small
Field of view	68.5 deg (total) 14 deg (per camera)	115 deg	4.2 deg	> 108.4 deg
Scrambler	Meris	Dual Babinet	Variant of Dual Babinet	Not yet defined
Scrambler position	Before instrument	Inside telescope	Inside telescope	Inside telescope
Scrambler illumin.	Collimated	Weakly converging, chief ray at +/-15deg	Converging F/2.7, normal chief ray	Not yet defined

Ideally, a polarization scrambler must be placed in front of the instrument, so that only depolarized light is collected, and the polarization sensitivity of all instrument subparts virtually plays no role in the measurement. Scramblers are built by assembling wedges of a birefringent crystal, e.g. quartz, in a way that the resulting component is chromatically corrected. Scramblers are traditionally understood as imposing polarization dependent phase delays that vary over the pupil so that the exiting polarization state depends on pupil position (x,y). Then, summing all the contributions averages out the Stokes parameters Q, U and V [7].

Alternatively, scramblers can be described as a set of cascaded polarization beamsplitters. Let us consider a collimated beam (fig. 2) with an arbitrary polarization state, that is incident on some optical instrument. If a single polarization beamsplitter is placed in the beam before the instrument, two polarization states with a variable repartition of energy are obtained. If, in addition, a second polarization beamsplitter is used, having its axis turned by 45 degrees, the instrument is still illuminated by two polarization states but now with a constant repartition of energy. This configuration is the basis of the scrambler design, and makes the instrument insensitive to the incident polarization. This intuitive picture also demonstrates the unavoidable degradation of image quality imposed by the scrambler. With a collimated beam, polarization scramblers create an image with 4 spots arranged in the shape of a parallelogram. On one side, for a better image quality it would be desirable to reduce the size of this parallelogram and have a single spot, but if the 4 spots are recombined then the depolarization power reduces to zero. In practice, depolarization can never be perfect, the image quality is always slightly degraded and a trade-off has to be made between both. Optimizing a scrambler is often a matter of finding the particular design which offers the largest margin for this trade-off.
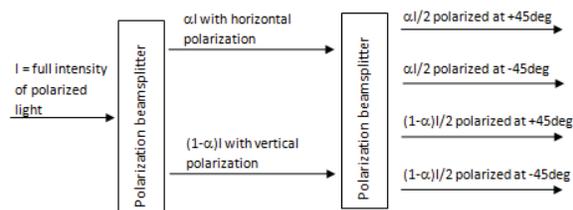

Figure 2. Working principle of a fully depolarizing scrambler, described with polarization beamsplitters (PBS). The full intensity after two PBS is I/2 polarized at +45 degrees, and I/2 polarized at -45 degrees.

The paper is arranged as follows. In section II, we describe the formulation of instrument requirements used for Sentinel-4 and 5 to constrain the polarization errors. Then the two most important scrambler designs called "Meris" and "Dual Babinet" are presented and compared. In section III, we discuss important instrumental aspects influencing the optimisation of the polarization performance for S4 and S5: position of the scrambler in the instrument, use of the instrument symmetries, use of a scrambler in a converging beam or at large incidence angles, and finally polarization dependent pointing errors.

II. SPECIFICITIES OF ATMOSPHERIC MISSIONS

A. Constraints on the polarization errors

Assuming that the instrument response to polarization can be described with the Mueller formalism, we can describe briefly the impact of polarization errors. If the observed Earth radiance $R(\lambda)$ has a degree of polarization DOP(λ) and a direction of linear polarization θ, the corresponding intensity detected by the instrument is:

$$S(\lambda,\theta) = R(\lambda)M_{11}(\lambda) \begin{bmatrix} 1 + \dfrac{M_{12}(\lambda)}{M_{11}(\lambda)} DOP(\lambda)\cos(2\theta) \\ + \dfrac{M_{13}(\lambda)}{M_{11}(\lambda)} DOP(\lambda)\sin(2\theta) \end{bmatrix}. \quad (1)$$

Polarization sensitivity is an estimate of the radiometric error due to the absence of knowledge of the polarization state of the measured input signal. It is calculated from the min and max signals measured when the instrument is illuminated with a fully polarized signal that can have any direction. We get a simple relation:

$$PS(\lambda) = \frac{\max\limits_{\theta} S(\lambda,\theta) - \min\limits_{\theta} S(\lambda,\theta)}{\max\limits_{\theta} S(\lambda,\theta) + \min\limits_{\theta} S(\lambda,\theta)} = \frac{\sqrt{M_{12}^2(\lambda) + M_{13}^2(\lambda)}}{M_{11}(\lambda)}. \quad (2)$$

TABLE II.   POLARIZATION REQUIREMENTS FOR MERIS, S4 AND S5.

instrument	band limits (nm)	PS requirement	RSRA requirement	window width
MERIS	390-1040	1%	-	-
S4	305-315	1%	0.1%	3 nm
	315-500	1%	0.05%	3 nm
	750-775	1%	0.05%	7.5 nm
S5	270-315	0.5%	0.1%	3 nm
	315-500	0.5%	0.05%	3 nm
	685-775	0.5%	0.05%	7.5 nm
	1590-1675	20%	0.16%	85 nm
	2305-2385	20%	0.3%	50 nm

Requirements for polarization sensitivity are similar for MERIS and the atmospheric missions S4 and S5, but it was soon realised that spectral oscillations in the instrument radiometric error can correlate with the absorption cross section of atmospheric target trace gases (e.g. NO_2). A new set of requirements was derived specifically for the atmospheric missions S4 and S5, aiming to constrain the possible spectral oscillations. Assuming that the instrument is measuring a target with a spectrally constant reflectance ρ_0, with $I(\lambda)$ being the irradiance:

$$\rho_0 = \frac{\pi R(\lambda)}{I(\lambda)}. \quad (3)$$

The measured reflectance $\rho(\lambda)$ is found by dividing the radiance measurement $S(\lambda)$ by the measured irradiance $I(\lambda)M_{11}(\lambda)$:

$$\rho(\lambda) = \rho_0 \frac{S(\lambda)}{R(\lambda)M_{11}(\lambda)}. \quad (4)$$

The following quantity, called Relative Spectral Radiometric Accuracy (RSRA), giving the peak-to-peak relative error within a specified window width, was then evaluated for $\rho(\lambda)$:

$$RSRA(\lambda) = \max_{\theta} \left[\frac{\max\limits_{\lambda \in \Delta\lambda} \rho(\lambda,\theta) - \min\limits_{\lambda \in \Delta\lambda} \rho(\lambda,\theta)}{\rho_0} \right]. \quad (5)$$

The requirement values that have been used for RSRA during both mission phases A are shown in table II. Polarization is only one contributor to RSRA, other possible contributions come from: speckles from the Sun calibration diffuser, straylight and detector effects. Calculating the RSRA according to equation (3) over a window of e.g. 3nm, is equivalent to applying a high pass filter rejecting the oscillations with periods larger than 6nm. This new figure RSRA(λ) cannot be deduced from the spectral variations of PS(λ). The reason becomes intuitive if $x=M_{12}/M_{11}$ and $y=M_{13}/M_{11}$ are interpreted as rectangular coordinates. Then PS(λ) is the radius $= sqrt(x^2+y^2)$ and to derive RSRA the spectral variations of both the radius and the polar angle atan(y/x) are needed. This new requirement turned out to be a design driver for S4 and S5 instruments.

B. Meris and Dual Babinet scramblers

MERIS (MEdium Resolution Imaging Spectrometer) onboard Envisat was the first Earth observing ESA mission to use a polarization scrambler. The MERIS scrambler is made of three cemented wedges, two in quartz and one in fused silica for chromatic correction (see fig.3). It depolarizes the input illumination very efficiently but it shows rapid spectral oscillations in its residual polarization sensitivity, which prevent its use for atmospheric measurements (see measured data in fig.4 and simulated data in fig.5).
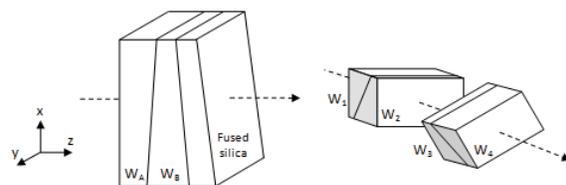

Figure 3.   Left : MERIS scrambler, right : Dual Babinet scrambler.

For each wedge in the MERIS scrambler, assuming that the thickness t depends on the pupil coordinates (x,y) with $t(x,y) = t_0 + \Delta t(x,y)$, t_0 being the thickness at pupil center, the phase difference between an ordinary ray and an extraordinary ray has the following form:

$$\Delta\varphi_{MERIS}(x,y) = \frac{2\pi}{\lambda}(n_e - n_o)\left[t_0 + \Delta t(x,y)\right]. \quad (6)$$
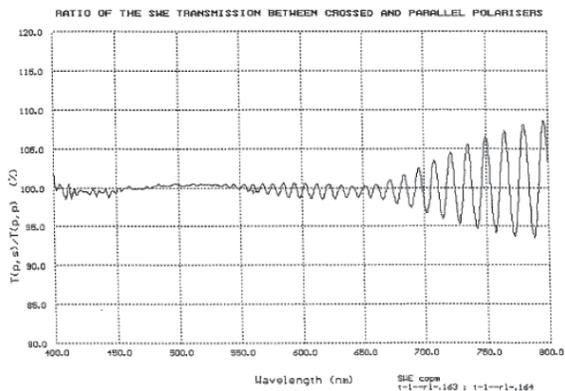
Figure 4. Ratio of measured intensities behind the MERIS scrambling window assembly (SWA) placed between crossed and parallel polarizers [8]. In this experimental result, the oscillations are smoothed by the measurement bandwidth of 5nm and then almost disappear around 500nm. The pupil is 20*40mm with 2 rounded corners.
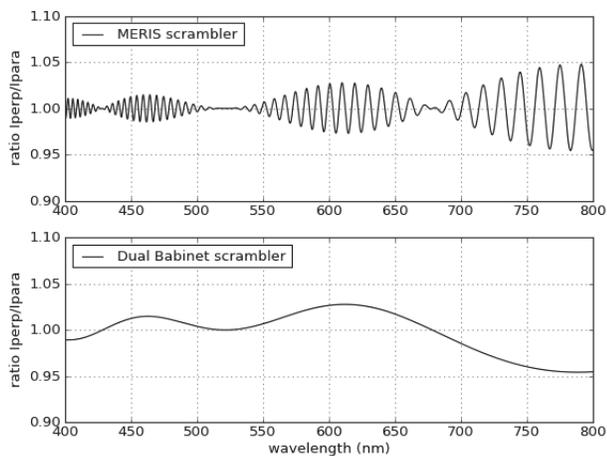

Figure 5. (top) Simulated ratio of measured intensities behind the MERIS scrambling window assembly (SWA) placed between crossed and parallel polarizers. No spectral smoothing is used, the simulated scrambler has a perfect rectangular pupil 20*40mm and wedge angles of 8mrad. (bottom) The simulation is repeated for an equivalent Dual Babinet with a wedge angle 4mrad : we recover the envelope of the MERIS oscillations.

This phase shift changes very rapidly with wavelength due to the large thickness t_0 divided by λ. This is the origin of the fast oscillations.

In the Dual Babinet scrambler, the wedges A and B of the MERIS design are each replaced by two wedges W1+W2 and W3+W4 with crossed axes such that the ordinary ray in W1 (resp. W3) becomes the extraordinary ray in W2 (resp. W4). In addition W1 and W2 (resp. W3 and W4) have opposite wedge angles so that the assemblies W1+W2 and W3+W4 have parallel external sides and there is no need for a chromatic correction (see fig.3). In the Dual Babinet the phase difference

between an ordinary ray and an extraordinary ray in the first pair of wedges becomes:

$$\Delta\varphi_{DB}(x, y) = \frac{2\pi}{\lambda}(n_e - n_o)2\Delta t(x, y). \qquad (7)$$

Due to the much smaller thickness involved in this expression, the fast spectral oscillations seen in the MERIS scrambler now disappear. This is illustrated on fig. 3, where the ratio of observed intensities between crossed and parallel polarizers are shown for both a MERIS and an equivalent Dual Babinet scrambler. For the Dual Babinet, all fast oscillations vanish and we recover the envelope of the curve observed for the MERIS scrambler.

III. S4 AND S5 INSTRUMENTS

A. Scrambler position in the instrument

Many optical components can contribute to the polarization sensitivity of the whole instrument. Typically, the most sensitive components are diffraction gratings, prisms, mirrors used at large incidence such as dichroics, scan or folding mirrors, and finally the telescope mirrors. Refractive elements are less sensitive to polarization as long as they are illuminated close to axis, as a result of their revolution symmetry.

In the MERIS instrument it was possible to place a scrambler in front of the complete instrument, thanks to the small pupil required for a low Earth orbit (LEO) instrument. Sentinel-4, which flies on a GEO orbit, has a pupil of 95mm and a large scan mechanism, which makes it impossible to use a Dual Babinet as the first component. For Sentinel-5, a very small pupil is expected, without a scan mirror. However the required field of view of 108.4 deg makes it difficult to achieve the phase shift compensation described in the previous section even with a Dual Babinet. If all 4 wedges have the same center thickness for nadir observation, this is no longer true at the edge of the swath due to the strongly tilted incident beams. Additionally, specific effects occurring at large incidences, discussed in section III.D, will also create spectral oscillations.

For these reasons, implementing a scrambler inside the instrument seems necessary for S4 and S5. As a consequence, other mitigation methods are required to compensate the polarization sensitivity of the scan mirrors and first optical components placed before the scrambler. A possibility is to use thin tilted plates with one uncoated surface, which then introduce different losses for each polarization component. These compensating plates were first suggested in [9] and are used in the S4 instrument. For designs with folding mirrors, another possibility is to combine them by pairs so that s polarization on one becomes p on the other and vice-versa, in order to achieve a compensation.

B. Use of the instrument's symmetries

It can be noted that the Dual Babinet scrambler is made of two successive HV depolarizers, the second one being rotated by 45 degrees. HV depolarizers are depolarizing only one linear state, as described in [10]. The following result is actually valid for both the MERIS and the Dual Babinet

scramblers: the depolarization of incoming linear states at 0 deg (Stokes parameters (I,Q,U,V)=(1,1,0,0)) or 45 deg (Stokes parameters (I,Q,U,V)=(1,0,1,0)) is achieved by different wedges, respectively W1+W2 (or WA) and W3+W4 (or WB).

When designing a polarization scrambler for a given instrument, the temptation is high to identify the axis of highest polarization sensitivity of the instrument, then strongly depolarize along this axis, and use a weaker (or even no) depolarization power along the other axis. In general the direction of highest sensitivity is imposed by the spectrometer's grating, and corresponds to linear states oriented along slit and across slit. Such a solution has been considered for the phase A scrambler design of the S4 instrument (further discussed in next section). However we point out that the approach bears considerable risk. Experience shows that the instrument always has some non negligible sensitivity to the +45/-45deg linear states, even if this should not be the case according to its symmetries. Such unexpected dependency has been observed in SCIAMACHY and Gome-2 [11]. Its explanation is not clear, it may be explained e.g. by stress induced birefringence. Based on this observation it was decided to use a fully depolarizing scrambler (Dual Babinet) for the OMI instrument, although the instrument symmetry could indicate that a HV polarizer was sufficient.

C. Scrambler in converging beam

During the phase A of Sentinel-4, a Dual Babinet scrambler was proposed, having the wedge angle of W3 and W4 set to 0 deg. This scrambler is thus composed of a HV depolarizer, followed by a set of two birefringent plates having their crystal axes at +/- 45 deg from the axes of the HV depolarizer. If this scrambler would be placed in a collimated beam, it would only depolarize one linear Stokes parameter (Q or U). In the S4 design, it was placed inside the telescope, in the converging beam (F/2.7 or F/3.6 depending on the spectral band). Then the first pair of wedges, aligned with the axis of polarization sensitivity of the grating, is strongly depolarizing, while the second pair is weakly depolarizing.

This weak depolarization generated by the wedges W3+W4 is only possible thanks to the converging beam. To understand it, one has to note that the concept of a polarization scrambler based on wedges is introducing a polarization dependent tilt. It is in principle possible to depolarize by introducing any other polarization dependent aberration. In the S4 scrambler, the pair of parallel plates W3+W4 is introducing a polarization dependent defocus, plus an astigmatism for the extraordinary ray due to the dependency of the extraordinary index with the propagation direction [10, 12]. Due to these polarization dependent aberrations, we obtain different spots in the focal plain, which are overlapping but still have different shape so that the "recombination" which would cancel the scrambling effect does not take place, or at least not efficiently.

The performance of this Sentinel-4 scrambler with two parallel plates is shown on figure 6. On the left side, we see two curves which correspond to the polarization sensitivities obtained for two incoming linear polarization states, aligned with the axes of strongest or weakest depolarization. The use of

other polarization-dependent aberrations than tilt opens the door to new possible designs for polarization scramblers.
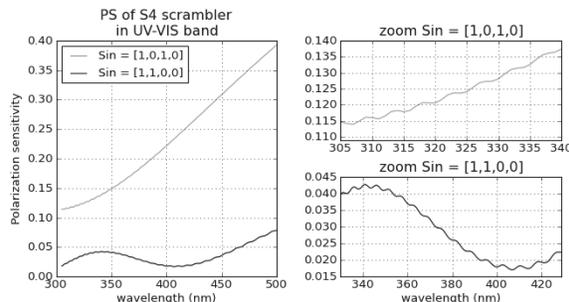

Figure 6. Calculated polarization sensitivity for the scrambler design of Sentinel-4 phase A. The instrument is replaced with a linear polarizer having the worst case orientation. Left : PS curves for polarization states along the axes of strong (black) and weak (gray) depolarization. Right : zoom showing the spectral oscillations in the PS curves.

D. Illumination at large angles of incidence

When a polarization scrambler is illuminated at large angles of incidences, new effects appear, which are discussed now. Using the coordinate system defined on fig. 3, we assume an incident beam that travels inside the scrambler wedge W1 with an incidence angle ψ, along the direction **u**, and arrives at the interface between W1 and W2. The crystal axes of the wedges W1 and W2 have the azimuths α_1 and α_2 and are defined by:

$$\mathbf{u} = \begin{pmatrix} sin\,\psi \\ 0 \\ cos\,\psi \end{pmatrix}, \quad \mathbf{axis}_1 = \begin{pmatrix} cos\,\alpha_1 \\ sin\,\alpha_1 \\ 0 \end{pmatrix}, \quad \mathbf{axis}_2 = \begin{pmatrix} cos\,\alpha_2 \\ sin\,\alpha_2 \\ 0 \end{pmatrix}. \quad (8)$$

As we will show, due to its non-normal incidence, at the interface the beam sees the crystal axis of W2 at a slightly different angle than α_2. The corresponding small rotation has direct consequences on the depolarization power and spectral oscillations generated by the scrambler. Illumination of a scrambler at large angles of incidence is directly relevant for LEO instruments such as Sentinel-5 due to their large fields of view, but also for configurations with a scrambler illuminated by a converging beam (e.g. Sentinel-4): in such case, non-normal angles are found with all possible azimuths.

According to Lekner [13] the directions of the electric fields corresponding to the ordinary and extraordinary beams are, in the limit of a small birefringence $n_o \sim n_e$ valid for quartz:

$$\mathbf{e}_{O1} = N_1 \begin{pmatrix} -\sin\alpha_1 \cos\psi \\ \cos\alpha_1 \cos\psi \\ \sin\alpha_1 \sin\psi \end{pmatrix}$$

$$\mathbf{e}_{E1} = N_1 \begin{pmatrix} \cos\alpha_1 \cos^2\psi \\ \sin\alpha_1 \\ -\cos\alpha_1 \sin\psi \cos\psi \end{pmatrix} \tag{9}$$

where N_1 is a normalisation constant, and similar expressions hold for the electric field directions in W2. The projection of the electric fields in W1 onto the electric fields in W2, which occurs at the interface W1/W2, is described by:

$$\begin{pmatrix} E_{O2} \\ E_{E2} \end{pmatrix} = \begin{pmatrix} \mathbf{e}_{O1}\cdot\mathbf{e}_{O2} & \mathbf{e}_{E1}\cdot\mathbf{e}_{O2} \\ \mathbf{e}_{O1}\cdot\mathbf{e}_{E2} & \mathbf{e}_{E1}\cdot\mathbf{e}_{E2} \end{pmatrix} \begin{pmatrix} E_{O1} \\ E_{E1} \end{pmatrix}$$

$$= \begin{pmatrix} \cos\Delta\alpha & -\sin\Delta\alpha \\ \sin\Delta\alpha & \cos\Delta\alpha \end{pmatrix} \begin{pmatrix} E_{O1} \\ E_{E1} \end{pmatrix} \tag{10}$$

$$\tan\Delta\alpha = \frac{\sin(\alpha_2 - \alpha_1)\cos\psi}{\sin\alpha_1 \sin\alpha_2 + \cos\alpha_1 \cos\alpha_2 \cos^2\psi} \tag{11}$$

$$\neq \tan(\alpha_2 - \alpha_1)$$

where E_{O1}, E_{E1}, E_{O2} and E_{E2} are the electric field complex amplitudes of the beam. We see that the Jones matrix of the interface W1/W2 is a rotation matrix, with an angle slightly different from $\alpha_2-\alpha_1$. The deviation between the apparent angle $\Delta\alpha$ and the true angle $\alpha_2-\alpha_1$ is a known effect (see e.g. [14]) but its implications on the performance of polarization scramblers has apparently not been recognized.

In fig. 7 below, we plot $\Delta\alpha$ as a function of the incidence angle for crystal axes at $\alpha_2-\alpha_1=45$ deg (representative of the W2/W3 interface in a Dual Babinet). The most favourable situation occurs for $\alpha_1=22.5$ deg, where the apparent angle is very close (but not equal) to 45deg in all situations. For other azimuth orientation, the apparent angle $\Delta\alpha$ deviates from the true angle $\alpha_2-\alpha_1$ by up to 15 degrees at large incidence angles $\psi=45$deg. For crystal axes at $\alpha_2-\alpha_1=90$ deg (representative of the W1/W2 and W3/W4 interfaces in a Dual Babinet) similar curves can be calculated. In this case the condition $\alpha_2-\alpha_1=\Delta\alpha$ is exactly met for $\alpha_1=0$deg or $\alpha_1=90$deg, as can be proven using equation (11). Nevertheless this circumstance cannot be used for the W1/W2 interface in a Dual Babinet because then the interface W3/W4 is placed at the most unfavourable angle $\alpha_1=\pm45$deg. Once again, the difference between apparent angle $\Delta\alpha$ and true angle $\alpha_2-\alpha_1$ can be significant at large incidence angles.

This effect has the following consequences for a Dual Babinet : at the interfaces W1/W2 and W3/W4, a deviation from $\alpha_2-\alpha_1=90$ deg means that additional weak beams are generated, for which the compensation of the optical paths specific to this

design is no longer achieved. The additional beams then create spectral features as in the MERIS scrambler concept. Other effects that occur with illumination at large angles, such as the increase of optical path due to tilted path, or the change of extraordinary index with propagation direction, will only slightly impact the compensation condition and cannot generate fast oscillations. The oscillations can be seen on fig. 8 below, where the polarization sensitivity of a Dual Babinet is plotted for various incidence angles. The scrambler has wedges of 1deg, a square spot pattern and crystal axes $\alpha_1=0$deg, $\alpha_2=90$deg, $\alpha_3=+45$deg and $\alpha_4=-45$deg. The pupil is circular with diameter 30mm, all wedges are made of quartz and have 4mm thickness at pupil center. The incident parallel beams have 0 deg (normal) and 20deg incidence, and lie within the (x,z) plane of fig. 3.
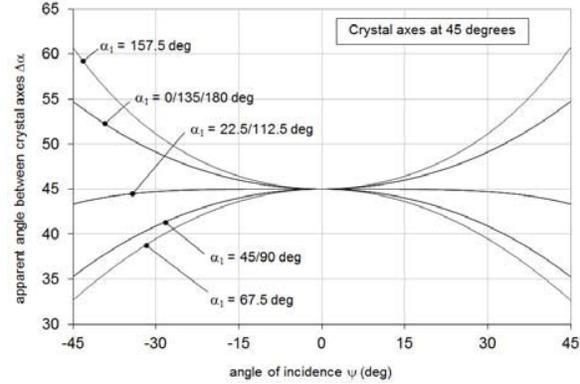
Figure 7. Deviation between the apparent angle $\Delta\alpha$ and true angle α_1-α_2 between the crystal axes at the W2/W3 interface in a Dual Babinet scrambler.
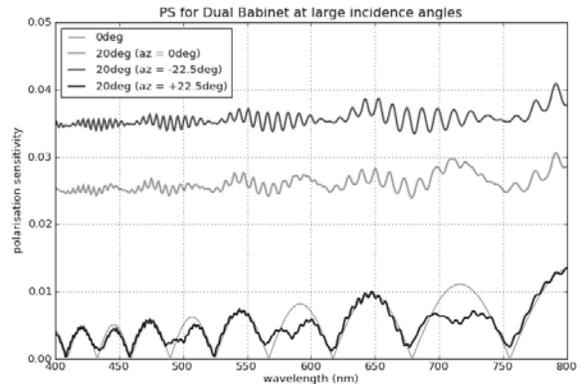
Figure 8. Polarization sensitivity of a Dual Babinet scrambler illuminated at normal and 20 deg incidence and rotated azimuthally. For each curve, the instrument is replaced with a linear polarizer having the worst case orientation. The PS curve is the strongest at an azimuth of -22.5 deg (consistent with $\alpha_1=157.5$ deg on fig. 7), and becomes the lowest at an azimuth of +22.5 deg (consistent with $\alpha_1=22.5$ deg on fig. 7). The fast oscillations result from the deviation from 90deg of the apparent angle between the crystal axes at the interfaces W1/W2 and W3/W4.

Additional curves have been calculated for the same scrambler that was rotated by various angles and also show the oscillations. The uncompensated beams also explain the small oscillations observed in the PS curves calculated for the S4 scrambler, on fig. 6.

The angle of 45 deg between crystal axes at the interface W2/W3 is essential and any deviation may strongly decrease depolarization efficiency. As seen from fig. 8, the level of polarization sensitivity strongly depends on the scrambler azimuth position. As expected from fig. 7 the best configuration is achieved for α_1= 22.5 deg and the worst one for α_1 = -22.5 deg. In principle it is possible to optimise the azimuthal position of the scrambler to minimise polarization sensitivity. It turns out that the residual polarization in the beam after the scrambler, created by this effect, has a well defined direction that can be conveniently oriented at 45 deg with the polarization axes of the spectrometer grating. In practice, such optimisation is done automatically with a numerical model, replacing the spectrometer with a partial polarizer and searching the best scrambler parameters. The above analysis may help to understand better the performance and compare candidate designs.

E. Polarization dependent pointing

Another effect which deserves attention is the polarization dependent pointing of the scrambler, which creates a co-registration error. When the linear polarization of the incident beam rotates, the pattern observed in a focal plane after the scrambler is slightly moving. For a Dual Babinet, if the input beam is unpolarized, all 4 spots receive equal intensity. If now the incident beam is linearly polarized, depending on the polarization direction 2 spots will be illuminated, or, if the polarization state is rotated by 90 degrees all the intensity will move towards the two opposite spots, giving a different position to the image barycentre.

Let us illuminate a Dual Babinet scrambler with a collimated beam on axis. If a lens with focal length f is placed behind it, the positions of the 4 spots in the focal plane are:

$$\begin{pmatrix} x_{spot} \\ y_{spot} \end{pmatrix} = \pm f \Delta n \sigma_1 \begin{pmatrix} \cos \beta_1 \\ \sin \beta_1 \end{pmatrix} \pm f \Delta n \sigma_3 \begin{pmatrix} \cos \beta_3 \\ \sin \beta_3 \end{pmatrix} \quad (12)$$

where $\Delta n = n_e - n_o$ is the birefringence of the scrambler material, and the other parameters describe the variations of the thickness of wedge Wi with pupil coordinates (x,y):

$$t_i(x, y) = t_0 + (x \quad y) . \left[\sigma_i \begin{pmatrix} \cos \beta_i \\ \sin \beta_i \end{pmatrix} \right]$$

$$= t_0 + \sigma_i (x \cos \beta_i + y \sin \beta_i). \quad (13)$$

with σ_i being the wedge slope and β_i the wedge azimuth. For the Dual Babinet we have in particular $\sigma_1 = \sigma_2$, $\sigma_3 = \sigma_4$, $\beta_2 = \beta_1 + 180\text{deg}$ and $\beta_4 = \beta_3 + 180\text{deg}$.

The changing distribution of energy between the spots is easily understood by considering the "cascaded polarization beamsplitter" interpretation of the scrambler's mechanism (see fig.2). It can be calculated analytically. If the crystal axes azimuths of W1/W2/W3/W4 (as defined in section 2.4) are α_1=0 deg, α_2=90 deg, α_3=+45 deg and α_4=-45 deg, we get:

$$\begin{pmatrix} x_{barycenter} \\ y_{barycenter} \end{pmatrix} = f \Delta n \sigma_1 \begin{pmatrix} \cos \beta_1 \\ \sin \beta_1 \end{pmatrix} \cos(2\theta)$$

$$+ f \Delta n \sigma_3 \begin{pmatrix} \cos \beta_3 \\ \sin \beta_3 \end{pmatrix} \sin(2\theta) \quad (14)$$

$$\left\langle \cos\left[\frac{4\pi}{\lambda} \Delta n \sigma_1 (x \cos \beta_1 + y \sin \beta_1) \right] \right\rangle_{\substack{pupil \\ average}}$$

where the direction of the input beam linear polarization makes an angle θ with x, and 90deg-θ with y. In this expression, we recognize the position of each of the 4 spots expressed above. The first term proportional to σ_1 is usually dominating, and gives the barycentre move of a perfect scrambler. The second term is smaller and is a correction accounting for the finite depolarization power of the first pair of wedges. As we see from the equation, if the wedge angle σ_1 would tend to zero, the first pair of wedges W1+W2 would not depolarize and the barycentre shift would be imposed by the second pair of wedges W3+W4, in a different direction.

In practice, it is possible to modify the Dual Babinet design to correct for the first order shift (first term). One possibility could be to replace the wedged interface between W1/W2 by a spherical interface. Then, rather than separating two pairs of spots laterally on the focal plane, different defocus aberrations are introduced so that the separation is done axially. This comes at the cost of a lower depolarization efficiency, which unfortunately results in an increase of the second order shift (second term). Other approaches are under investigation for Sentinel-5.

IV. CONCLUSION

This paper summarizes design rules and performance aspects of polarization scramblers, identified by ESA during the phases A/B1 of the Sentinel-4 and Sentinel-5 missions. Despite their apparent simplicity, polarization scramblers show many complex effects which need to be analysed and considered during the instrument design phases. This paper documents the most important findings in support to future atmospheric missions. The simulations have been done with a scrambler model developed by EADS Sodern. Some of the effects will be investigated experimentally by EADS Sodern in the context of the breadboarding of the phase A scrambler design for Sentinel-4.

We thank the teams from Astrium GmbH and Kayser-Threde, industrial primes involved in the preliminary phases of Sentinel-4 and 5 for their availability and the stimulating discussions about polarization scramblers.

REFERENCES

[1] G.Bazalgette Courrèges-Lacoste, B.Ahlers, B.Guldimann, A.Short, B.Veihelmann and H.Stark, "The Sentinel-4/UVN instrument on-board MTG-S", Proc. of 2011 EUMETSAT Met. Sat. Conf., p. 59, 5-9 Sept. 2011, Oslo, Norway.

[2] G. Lichtenberg et al., "SCIAMACHY Level 1 data: calibration concept and in-flight calibration", Atmos. Chem. Phys., vol. 6, pp. 5347–5367, 2006.

[3] M. Gottwald, H. Bovensmann et al., "SCIAMACHY, Monitoring the Changing Earth's Atmosphere"; Published by DLR, 2006. Available at http://atmos.caf.dlr.de/projects/scops/sciamachy_book/sciamachy_book.html.

[4] J. Callies, E. Corpaccioli, M. Eisinger, A. Hahne and A. Lefebvre, "GOME-2 – Metop's Second-Generation Sensor for Operational Ozone Monitoring", ESA bulletin 102, May 2000.

[5] M. Rast, J. L. Bezy and S. Bruzzi, " The ESA Medium Resolution Imaging Spectrometer MERIS: a review of the instrument and its mission", Int. J. Remote Sensing, vol. 20, pp. 1681-1702, 1999.

[6] M. Dobber et al., "Ozone monitoring instrument calibration", IEEE Trans. Geos. Rem. Sensing, vol. 44, pp. 1209-1238, 2006.

[7] J. McGuire and R. Chipman, "Analysis of spatial pseudodepolarizers in imaging systems", Optical Engineering, pp. 1478-1484, 1990.

[8] Document provided by EADS Sodern, who performed the characterisation of the MERIS scrambling window assembly (SWA).

[9] E. Waluschka, P. Silvergate, C. Ftaclas and A. Turner, "Polarization sensitivity analysis of an Earth remote sensing instrument: the MODIS-N Phase B study", Proc. SPIE, vol.1746 Polarization analysis and Measurement, pp. 96-103, 1992.

[10] S. McClain, R. Chipman and L. Hillman, "Aberrations of a horizontal-vertical depolarizer", Applied Optics, pp. 2326-2331, 1992.

[11] See e.g. ref [3] section 5.5 where plots of the sensitivity to +45/-45 deg polarization of SCIAMACHY are shown. In the nadir mode, where the instrument symmetries would suggest no sensitivity, deviation of dzeta from 1.0 by about 20% is observed in the range 400-500nm, and higher values are seen at other wavelengths.

[12] M. Simon, "Image formation through monoaxial plane-parallel plates", Applied Optics, pp. 4176-4182, 1988.

[13] J. Lekner, "Reflection and refraction by uniaxial crystals", J.Phys.:Condens.Matter, vol3, pp. 6121-6133, 1991.

[14] J. Pezzaniti and R. Chipman, "Angular dependence of polarizing beam-splitter cubes", Applied Optics, pp. 1916-1929, 1994.